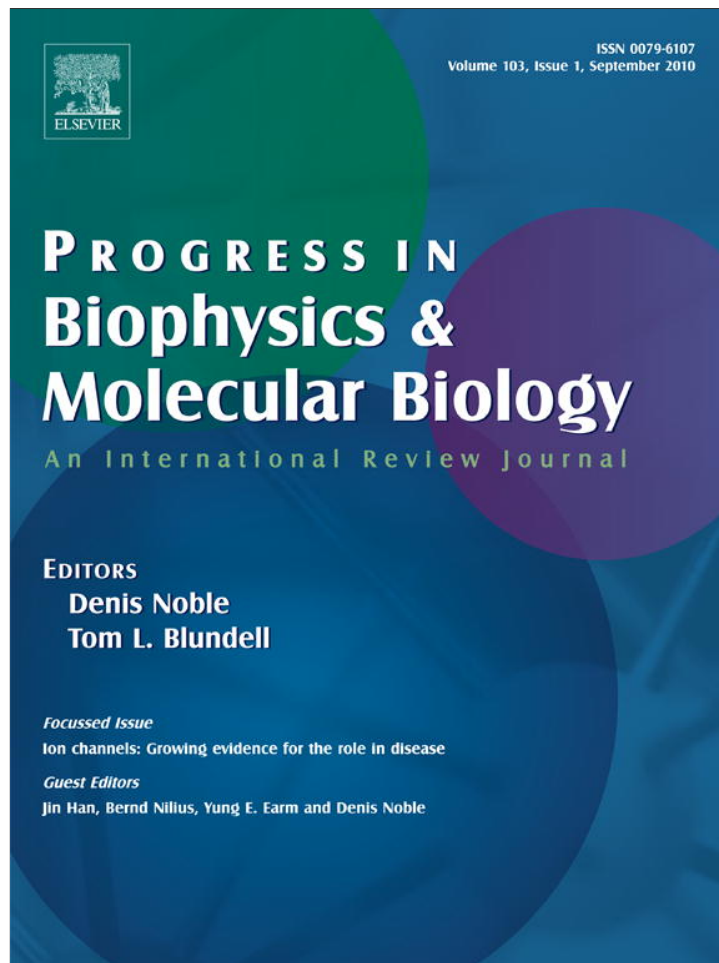


Provided for non-commercial research and education use.  
Not for reproduction, distribution or commercial use.



This article appeared in a journal published by Elsevier. The attached copy is furnished to the author for internal non-commercial research and education use, including for instruction at the authors institution and sharing with colleagues.

Other uses, including reproduction and distribution, or selling or licensing copies, or posting to personal, institutional or third party websites are prohibited.

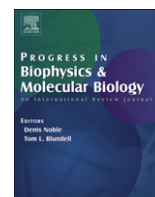
In most cases authors are permitted to post their version of the article (e.g. in Word or Tex form) to their personal website or institutional repository. Authors requiring further information regarding Elsevier's archiving and manuscript policies are encouraged to visit:

<http://www.elsevier.com/copyright>



Contents lists available at ScienceDirect

## Progress in Biophysics and Molecular Biology

journal homepage: [www.elsevier.com/locate/pbiomolbio](http://www.elsevier.com/locate/pbiomolbio)

## Review

Atrial local Ca<sup>2+</sup> signaling and inositol 1,4,5-trisphosphate receptorsJoon-Chul Kim<sup>a</sup>, Min-Jeong Son<sup>a</sup>, Krishna P. Subedi<sup>a</sup>, Yuhua Li<sup>a</sup>, Jung Real Ahn<sup>b</sup>, Sun-Hee Woo<sup>a,\*</sup><sup>a</sup> College of Pharmacy, Chungnam National University, 220 Gung-dong, Yuseong-gu, Daejeon 305-764, South Korea<sup>b</sup> Department of Physics, Sungkyunkwan University, Chun-Chun-dong 300, Suwon, South Korea

## ARTICLE INFO

## Article history:

Available online 1 March 2010

## Keywords:

Atrial myocytes

Ca<sup>2+</sup> signalingCa<sup>2+</sup> sparks

Inositol 1,4,5-trisphosphate receptor

subtype

HL-1 cell

RyR clustering

## ABSTRACT

In atrial myocytes lacking t-tubules, action potential triggers junctional Ca<sup>2+</sup> releases in the cell periphery, which propagates into the cell interior. The present article describes growing evidence on atrial local Ca<sup>2+</sup> signaling and on the functions of inositol 1,4,5-trisphosphate receptors (IP<sub>3</sub>R) in atrial myocytes, and show our new findings on the role of IP<sub>3</sub>R subtype in the regulation of spontaneous focal Ca<sup>2+</sup> releases in the compartmentalized areas of atrial myocytes. The Ca<sup>2+</sup> sparks, representing focal Ca<sup>2+</sup> releases from the sarcoplasmic reticulum (SR) through the ryanodine receptor (RyR) clusters, occur most frequently at the peripheral junctions in isolated resting atrial cells. The Ca<sup>2+</sup> sparks that were darker and longer lasting than peripheral and non-junctional (central) sparks, were found at peri-nuclear sites in rat atrial myocytes. Peri-nuclear sparks occurred more frequently than central sparks. Atrial cells express larger amounts of IP<sub>3</sub>R compared with ventricular cells and possess significant levels of type 1 IP<sub>3</sub>R (IP<sub>3</sub>R1) and type 2 IP<sub>3</sub>R (IP<sub>3</sub>R2). Over the last decade the roles of atrial IP<sub>3</sub>R on the enhancement of Ca<sup>2+</sup>-induced Ca<sup>2+</sup> release and arrhythmic Ca<sup>2+</sup> releases under hormonal stimulations have been well documented. Using protein knock-down method and confocal Ca<sup>2+</sup> imaging in conjunction with immunocytochemistry in the adult atrial cell line HL-1, we could demonstrate a role of IP<sub>3</sub>R1 in the maintenance of peri-nuclear and non-junctional Ca<sup>2+</sup> sparks via stimulating a posttranslational organization of RyR clusters.

© 2010 Elsevier Ltd. All rights reserved.

## Contents

1. Introduction .....	59
2. Atrial Ca <sup>2+</sup> signaling .....	60
2.1. Ca <sup>2+</sup> signaling and ultrastructure in atrial myocytes .....	60
2.2. Atrial Ca <sup>2+</sup> propagation on action potential .....	61
2.3. Atrial Ca <sup>2+</sup> sparks .....	61
3. IP <sub>3</sub> R in atrial myocytes .....	63
3.1. Expression and localization of IP <sub>3</sub> R subtypes in cardiac myocytes .....	63
3.2. Hormonal regulation of atrial Ca <sup>2+</sup> signaling via IP <sub>3</sub> R .....	63
4. Use of adult atrial cell line for genetic engineering to verify the role of IP <sub>3</sub> R subtype .....	63
4.1. Adult atrial cell line HL-1 .....	63
4.2. Characterization of spatio-temporal properties of Ca <sup>2+</sup> sparks in HL-1 cells .....	64
4.3. Loss of peri-nuclear Ca <sup>2+</sup> sparks in IP <sub>3</sub> R1 knock-down HL-1 cells .....	66
4.4. Possible role of IP <sub>3</sub> R1 in RyR clustering in atrial cells .....	68
5. Conclusions and future perspectives .....	69
Acknowledgements .....	69
References .....	69

## 1. Introduction

In the heart inositol 1,4,5-trisphosphate (IP<sub>3</sub>) is generated by many neurohumoral agonists including acetylcholine, endothelin (ET), catecholamines, prostaglandins (Hilal-Dandan et al., 1992), purines

\* Corresponding author. Tel.: +82 42 821 5924; fax: +82 42 823 6566.  
E-mail address: [shwoo@cnu.ac.kr](mailto:shwoo@cnu.ac.kr) (S.-H. Woo).

and angiotensin II (Puc at and Vassort, 1996; Goutsouliak and Rabkin, 1997) via the activation of phospholipase C (PLC), and it activates IP<sub>3</sub> receptors (IP<sub>3</sub>Rs) (Streb et al., 1983; Berridge, 2006), modulating cellular functions (Berridge, 2006; Berridge, 2009). IP<sub>3</sub>Rs are intracellular Ca<sup>2+</sup> release channels assembled from four large subunits, which are highly sensitized by increases in IP<sub>3</sub> concentration (Parker et al., 2004). IP<sub>3</sub>Rs are sensitive to Ca<sup>2+</sup> (Iino, 1990; Bezprozvanny et al., 1991; Finch et al., 1991), similar to ryanodine receptors (RyRs), and they require both IP<sub>3</sub> and Ca<sup>2+</sup> before they will open. There are three subtypes of IP<sub>3</sub>Rs (types 1, 2, and 3). Amongst IP<sub>3</sub>Rs the type 1 subtype (IP<sub>3</sub>R1) has attracted the most attention.

Normal rhythmical Ca<sup>2+</sup> signaling is mediated mainly by another Ca<sup>2+</sup> release channels RyRs in the heart. Recent evidence suggests that IP<sub>3</sub>R is an important modulator of Ca<sup>2+</sup> signaling and contractility and plays independent roles in cardiac cell functions under hormonal stimulations. This article will consider local aspects of atrial Ca<sup>2+</sup> signaling and potential role of IP<sub>3</sub>Rs in the control of local Ca<sup>2+</sup> releases in atrial cells.

## 2. Atrial Ca<sup>2+</sup> signaling

### 2.1. Ca<sup>2+</sup> signaling and ultrastructure in atrial myocytes

Contraction of mammalian cardiac myocytes is controlled by a sequence of events that include L-type Ca<sup>2+</sup> current (I<sub>Ca</sub>)-gated opening of Ca<sup>2+</sup> release channels (RyRs) in the sarcoplasmic reticulum (SR) (Beuckelmann and Wier, 1988; N bauer et al., 1989; Niggli and Lederer, 1990; Cleemann and Morad, 1991). During the action potential, Ca<sup>2+</sup> influx through the L-type Ca<sup>2+</sup> channels (dihydropyridine receptors, DHPRs) increases Ca<sup>2+</sup> concentration in the junctional space between the t-tubule or peripheral membrane and SR domain to open the RyRs on the SR membrane. The released

Ca<sup>2+</sup> from the SR in turn binds to the Ca<sup>2+</sup> sensing motif on the carboxyl-terminal of L-type Ca<sup>2+</sup> channel via calmodulin, which stops the Ca<sup>2+</sup> entry through the channel (Soldatov, 2003).

A clear difference in the ultrastructure between ventricular and atrial myocytes is in the t-tubular system. Unlike ventricular myocytes, the t-tubular system is either absent (Sommer and Waugh, 1976; Carl et al., 1995) or partially developed in atrial myocytes (Forssmann and Girardier, 1970; Ayetey and Navaratnam, 1978; Kirk et al., 2003; Woo et al., 2005). Therefore, most atrial myocytes have two functionally separate SRs; junctional SR close to the peripheral membrane and non-junctional (corbular) SR throughout the central regions of the cell with no associated cell membrane (Fig. 1C). In the peripheral junction, which is similar to the dyadic junction in the ventricular myocytes, the RyRs are found in close proximity to DHPRs (Carl et al., 1995), providing for cross-interaction between the Ca<sup>2+</sup> channels and RyRs (Fig. 1C). RyRs are also found in non-junctional or corbular SR throughout the central regions of the cell (Hatem et al., 1997; Mackenzie et al., 2001), with no associated DHPRs (Carl et al., 1995) (Fig. 1C). In fact, the mode of gating and the contribution of the non-junctional RyRs to cytosolic rise of Ca<sup>2+</sup> and the excitation–contraction coupling remain uncertain.

The distinct properties of ultrastructure and distribution of key Ca<sup>2+</sup> regulatory proteins in atrial myocytes have been reflected in whole-cell Ca<sup>2+</sup> transient on depolarization. In voltage-clamped human atrial myocytes, the activation of an L-type Ca<sup>2+</sup> channel elicited dome-shaped whole-cell Ca<sup>2+</sup> transient with an initial rapidly activating phase followed by a slowly activating phase (Hatem et al., 1997). Ryanodine, the inhibitor of RyR, blocked the whole-cell Ca<sup>2+</sup> transient by ~79% (Hatem et al., 1997) and slowed the inactivation of I<sub>Ca</sub> with the decrease of Ca<sup>2+</sup> releases in human atrial cells (Hatem et al., 1997), suggesting that the Ca<sup>2+</sup> transient

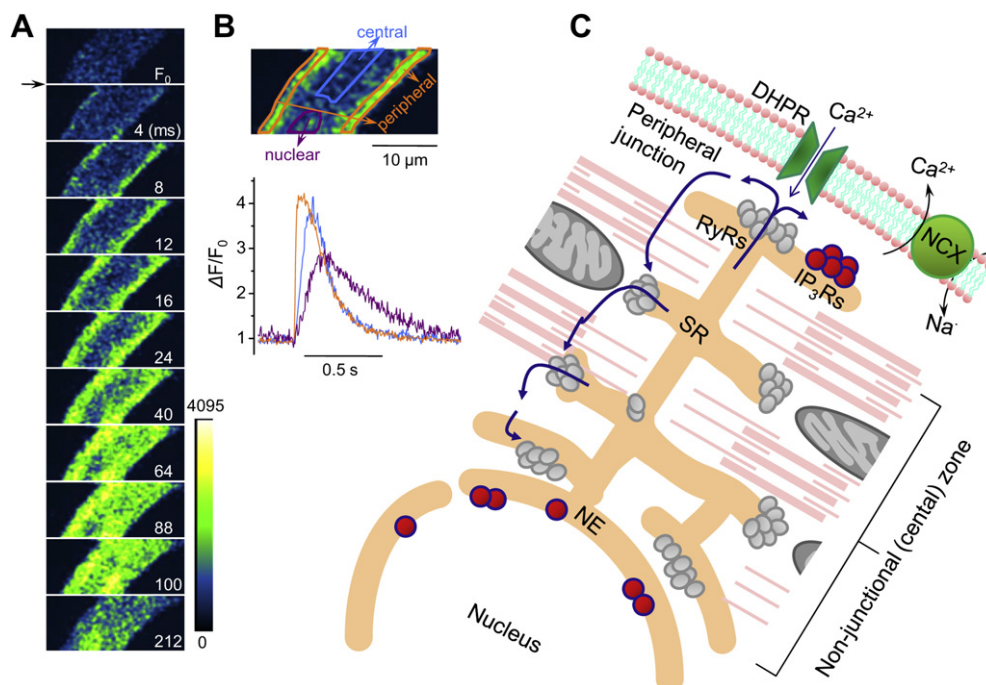


**Fig. 1.** Physiological Ca<sup>2+</sup> wave in atrial myocyte. (A) 2D Ca<sup>2+</sup> images measured at 4-ms interval with a rapid 2D confocal microscopy (A1, Nikon, Japan) during field stimulation (1 Hz) in a rat atrial myocyte, showing action potential-triggered transverse Ca<sup>2+</sup> propagation wave from peripheral junction to the cell interior. Atrial cells were isolated as previously described (Thu et al., 2006). Arrow indicates onset of depolarization. (B) Local Ca<sup>2+</sup> transients, measured in the peripheral, central, and nuclear regions of the confocal images, show delays of central and nuclear Ca<sup>2+</sup> transients. It is noted that a decay of nuclear transient is slower. (C) A model of atrial Ca<sup>2+</sup> signaling on action potential. Navy-colored arrows indicate Ca<sup>2+</sup>-induced Ca<sup>2+</sup> release in the peripheral junctional SR on the activation of DHPR, followed by a Ca<sup>2+</sup> diffusion-dependent sequential activations of the non-junctional Ca<sup>2+</sup> release sites (RyRs) in a saltatory mode (see text for more detail). DHPR: Dihydropyridine receptor. NCX: Na<sup>+</sup>-Ca<sup>2+</sup> exchanger. RyRs: Ryanodine receptors. IP<sub>3</sub>Rs: Inositol 1,4,5-trisphosphate receptors. SR: Sarcoplasmic reticulum.

was due essentially to SR  $\text{Ca}^{2+}$  release and that RyRs and DHPRs are functionally coupled.

Activation of RyRs in atrial cells was not entirely controlled by  $I_{\text{Ca}}$ . In the  $\text{Na}^+$ -containing  $\text{K}^+$ -rich internal solution, almost complete activation of the  $\text{Ca}^{2+}$  transient occurred before that of  $I_{\text{Ca}}$  (at  $-30$  mV, 74% of the  $\text{Ca}^{2+}$  transient), and for potentials above  $-10$  mV, the  $\text{Ca}^{2+}$  transient reached a plateau distinct from the bell-shaped voltage dependence of  $I_{\text{Ca}}$  (Hattem et al., 1997). On the other hand, in  $\text{Na}^+$ -free internal solution, a similar voltage relationship of the  $\text{Ca}^{2+}$  transient and  $I_{\text{Ca}}$  was obtained in human (Hattem et al., 1997) and rat atrial cells (Woo et al., 2002; Sheehan and Blatter, 2003). These reports suggest a significant contribution of the reverse  $\text{Na}^+$ - $\text{Ca}^{2+}$  exchange in the voltage dependence of  $\text{Ca}^{2+}$  transient in atrial myocytes.

## 2.2. Atrial $\text{Ca}^{2+}$ propagation on action potential

Simultaneous confocal  $\text{Ca}^{2+}$  imaging of peripheral and central  $\text{Ca}^{2+}$  signals in field-stimulated or voltage-clamped atrial myocytes revealed that  $\text{Ca}^{2+}$  release initiated at the cell periphery propagates into the interior of the myocyte (Fig. 1A and B) (Berlin, 1995; Hüser et al., 1996; Kockskämper et al., 2001; Mackenzie et al., 2001; Woo et al., 2002; Sheehan and Blatter, 2003). Dialysis of high concentrations of immobile  $\text{Ca}^{2+}$  buffer (1–2 mM EGTA) into patch-clamped rat atrial myocytes completely removed the  $I_{\text{Ca}}$ -triggered  $\text{Ca}^{2+}$  propagation wave (Woo et al., 2002), suggesting that the  $I_{\text{Ca}}$ -triggered  $\text{Ca}^{2+}$  propagation is mediated by  $\text{Ca}^{2+}$  diffusion from the cell periphery. However, the magnitude of central  $\text{Ca}^{2+}$  release is also dependent on the magnitude and duration of  $I_{\text{Ca}}$ , although the efficacy of  $I_{\text{Ca}}$  to trigger  $\text{Ca}^{2+}$  release in periphery of the myocytes was  $\approx 5$  times higher than in the center (Woo et al., 2002). Interestingly, the speed of  $\text{Ca}^{2+}$  propagation during  $I_{\text{Ca}}$  ( $\sim 230$   $\mu\text{m}/\text{s}$ ) was almost the same at different magnitudes of  $I_{\text{Ca}}$  (Woo et al., 2002), suggesting the existence of other regulatory mechanisms for the velocity of  $I_{\text{Ca}}$ -triggered  $\text{Ca}^{2+}$  propagation in addition to  $I_{\text{Ca}}$  and diffusion.

## 2.3. Atrial $\text{Ca}^{2+}$ sparks

Focal  $\text{Ca}^{2+}$  releases through the RyR clusters, “ $\text{Ca}^{2+}$  sparks” (Cheng et al., 1993), are thought to be elementary units for cytosolic  $\text{Ca}^{2+}$  releases in depolarized cardiac myocytes (Cheng et al., 1993; Cannell et al., 1994; Wier et al., 1994; Cleemann et al., 1998) and regulate contraction of nearby myofilaments. During action potential,  $I_{\text{Ca}}$  first activates peripheral junctional  $\text{Ca}^{2+}$  sparks in atrial myocytes (Kockskämper et al., 2001; Mackenzie et al., 2001; Woo et al., 2002; Fig. 1C), which is followed by a saltatory movement of the  $\text{Ca}^{2+}$  sparks into the cell interior (Woo et al., 2002).  $\text{Ca}^{2+}$  sparks also occur spontaneously in resting ventricular and atrial myocytes. Interestingly, the spontaneous sparks occur more often in the peripheral junctions (4- to 5-fold) than in the non-junctional cell interior (Woo et al., 2003a; Sheehan et al., 2006). Two-dimensional (2D) size of the peripheral and central sparks in atrial cells turned out to be the same (Woo et al., 2003a). Interestingly, analysis of 2D spark images, measured at more or less similar conditions, showed that atrial sparks (Woo et al., 2003a) were significantly larger and longer lasting than ventricular sparks (Cleemann et al., 1998). This suggests that the composition of atrial  $\text{Ca}^{2+}$  release units is significantly different from those of ventricular release units.

The precise mechanisms for the activation of spontaneous  $\text{Ca}^{2+}$  sparks and for higher propensity of peripheral junctional sparks in atrial myocytes are not clear. In fact, the SR  $\text{Ca}^{2+}$  contents in the peripheral and central regions were similar, and the peripheral and central spontaneous  $\text{Ca}^{2+}$  sparks were resistant to the blockade

of L-type  $\text{Ca}^{2+}$  current at resting membrane potential (Woo et al., 2003a). Direct interaction of RyR with the DHPR C-terminal LA motif via calmodulin at low resting  $\text{Ca}^{2+}$  concentration has been suggested to explain the higher propensity of spontaneous  $\text{Ca}^{2+}$  sparks in the periphery of atrial cells (Woo et al., 2003b). Such mechanism, however, may not explain the “eager sites” that show the highest frequency of spontaneous activity in some of the peripheral junctional sites (Mackenzie et al., 2001).

In rat atrial myocytes, we could also detect spontaneous  $\text{Ca}^{2+}$  sparks around the nucleus (“peri-nucleus”) in resting conditions (Fig. 2, “PNU”). The position of a peri-nuclear spark was confirmed by co-localizing the spark signal with syto-11 fluorescence in the same cell (Fig. 2B, upper image). Only cells free of  $\text{Ca}^{2+}$  waves were analyzed. Focal  $\text{Ca}^{2+}$  releases were automatically identified by a computerized algorithm in the “Pic” PC program (own written in C++). First, this algorithm subtracted the average background signal ( $F_0$ ) from the raw image along the  $x$  and  $y$  directions. If the pixel fluorescence ratio ( $F/F_0$ ) was  $\leq 0.3$  the signals became zero by low-pass filtering, whereas the signal brighter than the critical value remained intact. Then, the “groups” (“local maxima”), which were defined as connected non-zero signals, were identified as candidates of  $\text{Ca}^{2+}$  sparks. If the distance between a signal and a group is below a critical distance ( $\approx 1.2$   $\mu\text{m}$ ), the signal was included in the group. Then, if the number of signals in a group was  $> 5$ , we assigned the group as a real spark. To detect local maxima underneath the cell membrane, the extracellular space was excluded by setting up a mark at the cell border especially in 2D images (Woo et al., 2003a). The center of real spark, a position with maximal intensity in the group, was visualized in the image as a mark and exported as a coordinate (Fig. 4A and E).

To calculate frequency of sparks, central, peripheral, and peri-nuclear areas were directly measured by a PC program (EZ-C1, Nikon). The peri-nuclear region up to 1  $\mu\text{m}$  outside of the nucleus was considered as peri-nuclear area. The area up to 1.5  $\mu\text{m}$  immediately underneath the cell membrane was denoted as the peripheral domain. At a 30-Hz imaging speed to visualize the entire area of atrial myocytes, the frequency (events/ $10^3$   $\mu\text{m}^2$  s) of peri-nuclear sparks was  $2.83 \pm 0.81$  ( $n = 9$ ), which was 4.5-fold higher than that of central sparks ( $0.62 \pm 0.21$ ) but  $\sim 3$ -fold lower than the frequency of peripheral sparks ( $8.09 \pm 1.75$ ) (Fig. 2D). The difference ( $\sim 13$ -fold) between central and peripheral spark frequency became larger compared with the previous report (5-fold) obtained in a similar condition (Woo et al., 2003a) because of the separate consideration of peri-nuclear sparks from central sparks.

To compare the time course and unitary properties of peri-nuclear sparks with central or peripheral sparks, rapid (240 Hz) 2D confocal  $\text{Ca}^{2+}$  imaging was performed in rat atrial cells. At the spark center, identified by the program, Gaussian fitting was done in 2D using “Pic” program with the same algorithm previously described (Woo et al., 2003a). The amplitudes ( $F_1/F_0$ :  $F_1$  is the magnitude of Gaussian curve and  $F_0$  means the background fluorescence) of peri-nuclear sparks ( $0.84 \pm 0.09$ ,  $n = 55$ ) were smaller than those of central ( $1.27 \pm 0.17$ ,  $n = 129$ ) and peripheral ( $1.38 \pm 0.08$ ,  $n = 61$ ) sparks. Full durations at half-maximum amplitude (FDHM) of peri-nuclear, central, and peripheral sparks were  $38 \pm 2.3$  ms,  $31 \pm 1.7$  ms and  $49 \pm 1.2$  ms, respectively, indicating that peri-nuclear sparks last significantly longer than others ( $P < 0.01$ ). Mean widths (full width at half-maximum, FWHM) of peri-nuclear sparks ( $2.36 \pm 0.08$   $\mu\text{m}$ ,  $n = 55$ ) and peripheral sparks ( $2.31 \pm 0.28$   $\mu\text{m}$ ,  $n = 61$ ) were similar ( $P > 0.05$ ). Central sparks ( $2.08 \pm 0.13$   $\mu\text{m}$ ,  $n = 129$ ) were narrower than peri-nuclear and peripheral sparks ( $P < 0.05$ ). The distinguished spatio-temporal properties of peri-nuclear sparks suggest that peri-nuclear  $\text{Ca}^{2+}$  release units are functionally separate from central or peripheral  $\text{Ca}^{2+}$  release sites and may have distinct structure and gating mechanism.

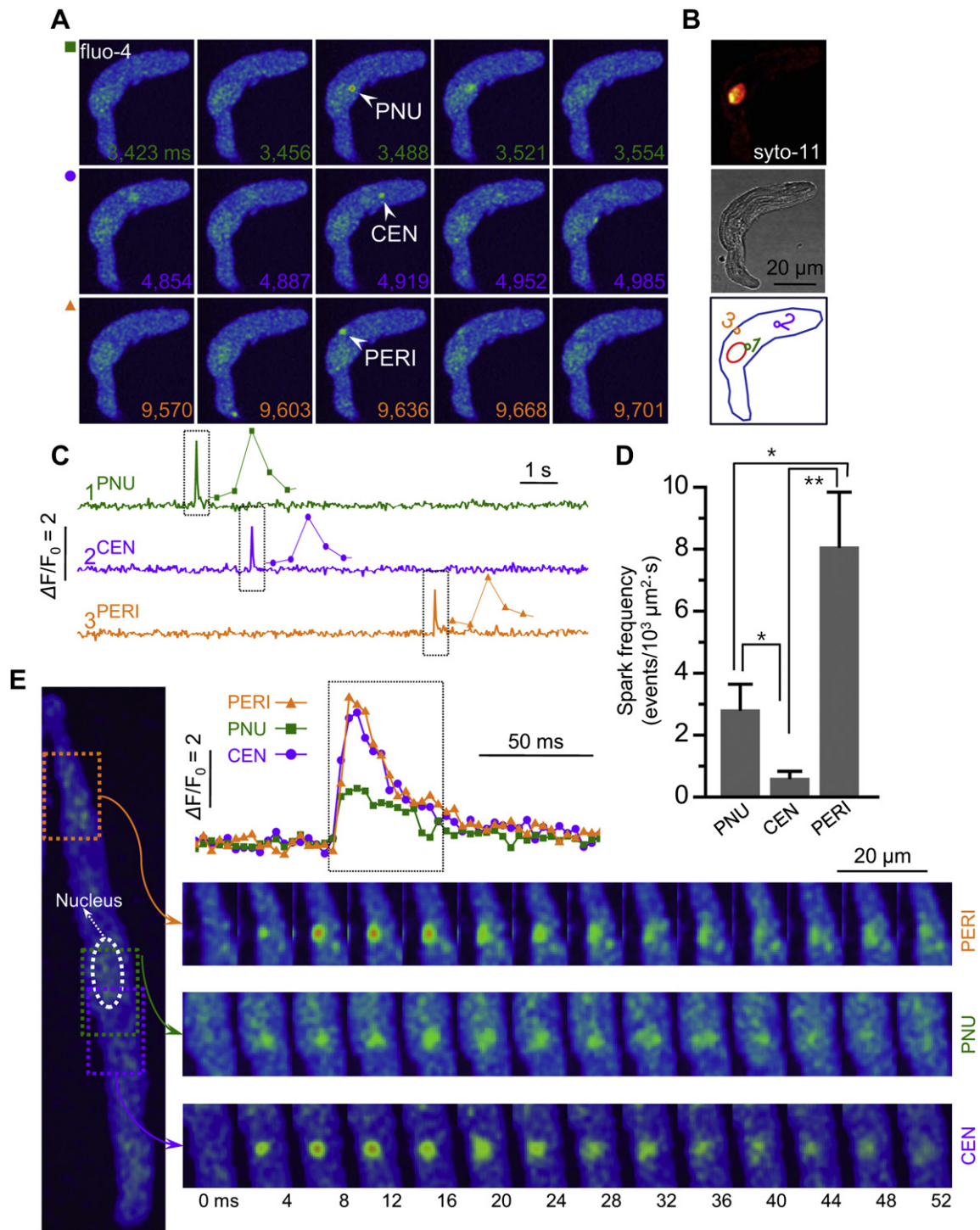


**Fig. 2.** Spontaneous peri-nuclear  $\text{Ca}^{2+}$  sparks in atrial myocytes. (A) Three series of 2D confocal fluo-4- $\text{Ca}^{2+}$  images show peri-nuclear (PNU), central (CEN), and peripheral (PERI) sparks recorded at 30 Hz in a rat atrial cell during the periods marked as boxes in panel C. Cells were loaded with  $3 \mu\text{M}$  fluo-4 AM for 40 min. (B) *Upper* image indicates confocal syto-11 fluorescence recorded from the same atrial cell, showing position of nucleus. *Lower* image shows three ROIs, where the numbered signal traces ( $F/F_0$ ) in the panel C were measured. Scatter plots above the traces in panel (C) represent expanded traces on  $x$  scale (time) from the boxed region. (D) Mean frequency of  $\text{Ca}^{2+}$  sparks in the peri-nucleus, center, and periphery.  $**P < 0.01$ ,  $*P < 0.05$  between two groups ( $n = 7$ ). (E) Developments and dissipations of peri-nuclear, central, and peripheral  $\text{Ca}^{2+}$  sparks in rat atrial myocytes. Sequential confocal  $\text{Ca}^{2+}$  images display representative sparks detected from the compartments (dotted boxes) at 240 Hz in the rat atrial cell, shown in the left side. *Inset* shows time courses of  $F/F_0$  measured from the focal region (diameter:  $1 \mu\text{m}$ ) of PERI, CEN, and PNU sparks.

### 3. IP<sub>3</sub>Rs in atrial myocytes

#### 3.1. Expression and localization of IP<sub>3</sub>R subtypes in cardiac myocytes

The expression levels of different IP<sub>3</sub>R subtypes vary in different regions of the heart (e.g., atrium, ventricle, and conduction tissue cells) and cardiac patients. The IP<sub>3</sub>R2 is the major subtype expressed in adult and neonatal ventricular myocytes (Bare et al., 2005; Luo et al., 2008). In atrial myocytes, the IP<sub>3</sub>R2 is also detected, of which expression is 6 to 10-fold higher than adult ventricular myocytes (Lipp et al., 2000). The IP<sub>3</sub>R1 was detected in atrial tissue (Yamada et al., 2001) and in rat Purkinje cells (Gorza et al., 1993). Furthermore, our own unpublished data showed significant expression of IP<sub>3</sub>R1 in isolated rat atrial myocytes (Kim et al., 2009). The expression of type 3 IP<sub>3</sub>Rs was not detectable in adult atrial cells (*data not shown*). The expression of IP<sub>3</sub>R1 is higher in human atrium having chronic atrial fibrillation (AF) (Yamada et al., 2001) and in the left ventricle of cardiomyopathic patients (by 123%) compared with normals (Go et al., 1995).

Subcellular localization of IP<sub>3</sub>Rs and the site of IP<sub>3</sub> generation seem to be very important to elicit specific physiological response in the local area of cells, because IP<sub>3</sub> generated by receptor activation or other mechanism is rapidly metabolized close to the site of release in cardiac cells (Woodcock and Matkovich, 2005). The precise localization of IP<sub>3</sub>R subtypes in cardiac myocytes is not fully understood. In rat ventricular myocytes, IP<sub>3</sub>R2 has been observed in the nuclear envelope (Bare et al., 2005) and t-tubules in small numbers (Mohler et al., 2005). In adult rat atrial myocytes, in sharp contrast, IP<sub>3</sub>R2 has been found at the peripheral junctional SR, with some co-localizations with type 2 RyR (RyR2) (Lipp et al., 2000). The precise localization of IP<sub>3</sub>R1, however, has not been successfully visualized by the immunocytochemistry, possibly because of a low density of IP<sub>3</sub>R1 in intact atrial cells.

#### 3.2. Hormonal regulation of atrial Ca<sup>2+</sup> signaling via IP<sub>3</sub>Rs

Cumulated evidence has demonstrated that IP<sub>3</sub> or IP<sub>3</sub>-producing hormones modulate atrial Ca<sup>2+</sup> signaling via IP<sub>3</sub>Rs. Maximum concentration of ET-1 (100 nM, 6–10 min) enhanced the magnitude of depolarization-induced Ca<sup>2+</sup> transients with some extra Ca<sup>2+</sup> releases (Lipp et al., 2000; Mackenzie et al., 2001; Zima and Blatter, 2004). It also induced delayed afterdepolarization (DAD) during diastole or Ca<sup>2+</sup> transient alternans in atrial cells (Mackenzie et al., 2002; Zima and Blatter, 2004). These effects were inhibited by 2-APB (2–5 μM), the blocker of IP<sub>3</sub>Rs. The arrhythmic Ca<sup>2+</sup> releases and larger Ca<sup>2+</sup> transients during ET-1 treatment were not observed in IP<sub>3</sub>R2 knock-out mouse atrial myocytes (Li et al., 2005), supporting a specific role of IP<sub>3</sub>R2.

The frequency of spontaneous Ca<sup>2+</sup> sparks is increased by activation of IP<sub>3</sub>Rs during the stimulation of ETR or α<sub>1</sub>-adrenergic receptor (AR) in atrial (Mackenzie et al., 2001; Zima and Blatter, 2004) and ventricular myocytes (Luo et al., 2008). In addition, direct application of IP<sub>3</sub> or its analogues enhanced resting Ca<sup>2+</sup> spark occurrences via IP<sub>3</sub>Rs in atrial cells (Lipp et al., 2000; Zima and Blatter, 2004). The enhancement of resting Ca<sup>2+</sup> spark occurrences and global Ca<sup>2+</sup> transients during the activation of ETR or α<sub>1</sub>-AR have been explained by the hypothesis that Ca<sup>2+</sup> release from the IP<sub>3</sub>R increases Ca<sup>2+</sup> in the vicinity of RyRs and enhances their activity via Ca<sup>2+</sup>-induced Ca<sup>2+</sup> release (Mackenzie et al., 2002; Zima and Blatter, 2004).

More recent functional evidence suggests that there may be IP<sub>3</sub>Rs in the nucleus of adult atrial myocytes. ET-1-induced enhancement of Ca<sup>2+</sup> transients was larger in the nucleus than the cytosol, and lower concentration (0.1 nM) of ET-1 selectively increased nuclear Ca<sup>2+</sup> transient via ET<sub>A</sub> receptor/IP<sub>3</sub>R signaling

pathway (Kockskämper et al., 2008). In cat atrial cells, application of IP<sub>3</sub> or an IP<sub>3</sub>R agonist, adenophostin, in permeabilized atrial cells caused an elevation of nuclear Ca<sup>2+</sup> concentration, which was sensitive to IP<sub>3</sub>R inhibitor (Zima et al., 2007).

Several groups have reported that diastolic Ca<sup>2+</sup> release may play a critical role in atrial pacemaker function (Lipsius et al., 2001) and in the activation of the Ca<sup>2+</sup>-dependent membrane ion channel or transporter (Lederer and Tsien, 1976; Lipp and Pott, 1988a; Lipp and Pott, 1988b; Hove-Madsen et al., 2004). Mackenzie et al. (2002) have suggested that arrhythmogenic action of agents cannot be linearly correlated with the ability to increase the intracellular global Ca<sup>2+</sup> rise or load, or sensitization of the Ca<sup>2+</sup> release mechanism. Digoxin increases basal Ca<sup>2+</sup> level and global Ca<sup>2+</sup> wave. However, the DAD is more frequent in the presence of ET-1 than in digoxin. Also isoproterenol enhances Ca<sup>2+</sup> transient and increase SR Ca<sup>2+</sup> load but hardly generates DAD (Mackenzie et al., 2002). Spontaneous Ca<sup>2+</sup> sparks were observed significantly more in the AF patients and they were associated with spontaneous inward Na<sup>+</sup>–Ca<sup>2+</sup> exchanger current that can depolarize the membrane potential (Hove-Madsen et al., 2004). It is known that the expression of atrial IP<sub>3</sub>R1 significantly increases in AF patients (Yamada et al., 2001). However, a precise subcellular signaling pathway linking the IP<sub>3</sub>R subtypes with a development of AF is not clear.

### 4. Use of adult atrial cell line for genetic engineering to verify the role of IP<sub>3</sub>R subtype

#### 4.1. Adult atrial cell line HL-1

An adult mouse atrial cell line called HL-1 has been widely used as a suitable adult atrial cell system to study atrial muscle structure and function *in vitro* using genetic engineering techniques (Claycomb et al., 1998). Although cultured embryonic and neonatal cardiac myocytes have also been widely used to study cardiac molecular physiology, they lack many characteristics of adult cardiac cells and are overgrown by non-myocytes after a few days in culture. HL-1 cells are the only cells available that continuously divide and retain an adult atrial phenotype in culture (Claycomb et al., 1998). These cells generate autorhythmic Ca<sup>2+</sup> transients at high confluence (Sartiani et al., 2002) and express key ion channels underlying action potential and Ca<sup>2+</sup>-induced Ca<sup>2+</sup> release (Claycomb et al., 1998). We have found that HL-1 cells express IP<sub>3</sub>R1 and IP<sub>3</sub>R2, very similar to adult rat atrial myocytes, and that IP<sub>3</sub>R1 and IP<sub>3</sub>R2 are localized to peri-nucleus and in the periphery, respectively (Kim et al., *in press*; Fig. 6C, WT). Compared with intact atrial myocytes, the expression of IP<sub>3</sub>R1 was higher in HL-1 cells (Kim et al., *in press*). Higher expression of peri-nuclear IP<sub>3</sub>R1 in HL-1 cells than in intact isolated atrial cells may suggest a more significant role of this subtype in the cell proliferation or autorhythmicity.

We adopted this atrial cell line to investigate the functional roles of IP<sub>3</sub>R subtypes in atrial local Ca<sup>2+</sup> signaling using an RNA interference technique, because a specific pharmacological inhibitor for each IP<sub>3</sub>R subtype is not available. Because it was not possible to directly use siRNA in intact adult cardiac myocytes, we screened several siRNA sequences using HL-1 cells to select suitable siRNA to null protein expression. To achieve this goal it was also necessary to characterize HL-1 cells in terms of local Ca<sup>2+</sup> signaling in advance, because there have been few studies on the spatio-temporal pattern of local Ca<sup>2+</sup> signal in this cell line.

We first tried to find if there is a t-tubule in HL-1 cells using di-8-ANEPPS, a membrane-specific fluorescence dye, but found no t-tubule (Fig. 3A). Immunolocalization using specific antibodies to the RyR2 revealed a somewhat disorganized arrangement of RyR2 in HL-1 cells (Fig. 3B) compared with very regular distributions of RyR2 with 2-μm intervals in intact mouse atrial myocytes (Fig. 3C). There

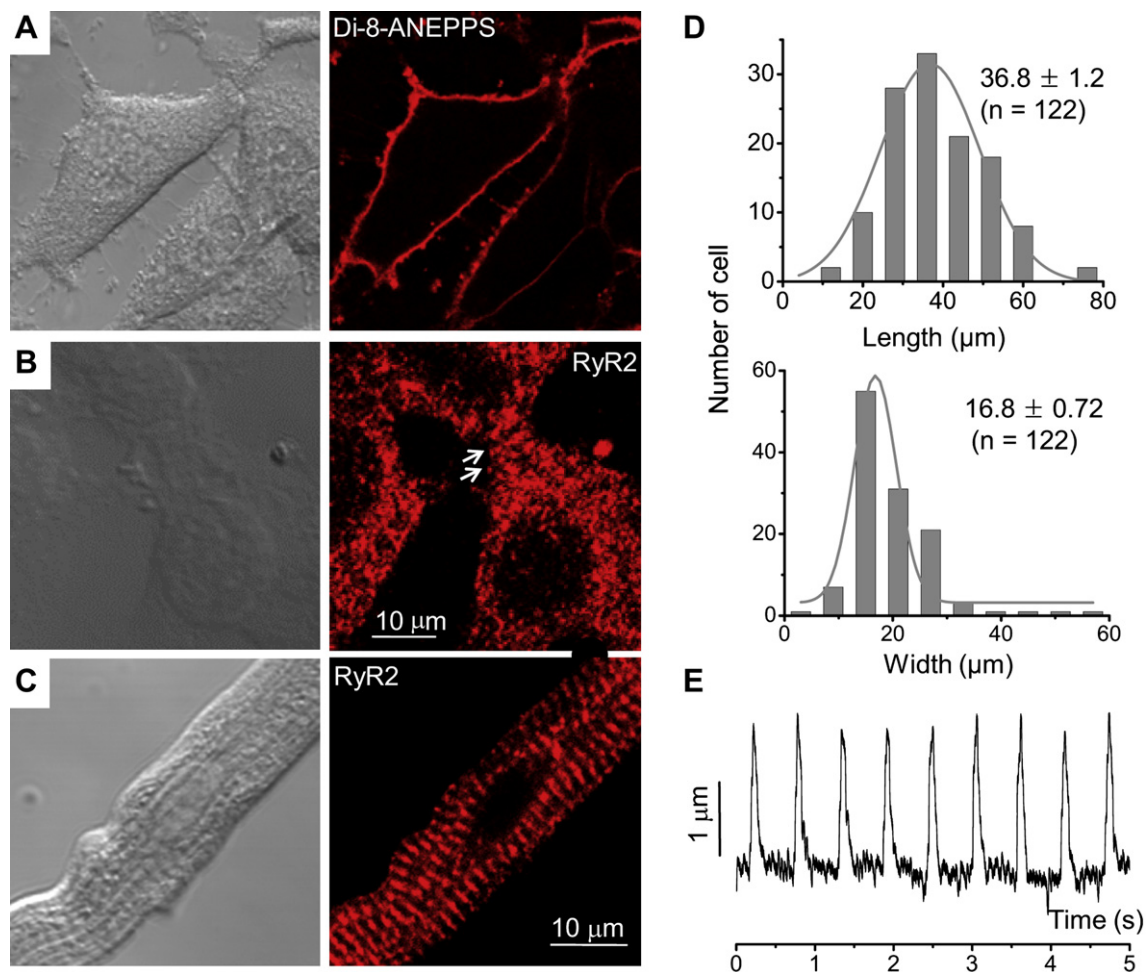


**Fig. 3.** Basic characteristics of adult mouse atrial cell line HL-1. *Left* images in panel (A–C): Transparent confocal image of HL-1 cells (A and B) and mouse atrial myocytes (C). *Right* image in A: confocal fluorescence image of di-8-ANEPPS (10  $\mu$ M di-8-ANEPPS for 5 min at RT), a cell membrane dye (Molecular Probes) shows no t-tubule. *Right* image in B and C: confocal image of type 2 ryanodine receptor (RyR2) immunofluorescence in HL-1 cells (B) and mouse atrial myocytes (C). (D) Distribution histogram showing length and width of HL-1 cell at >80% confluence. (E) Autorhythmic beating of HL-1 cell populations detected by video edge detector at 35  $^{\circ}$ C.

were some striping patterns of RyRs in some areas (see arrows, Fig. 3B). Immunofluorescence of the RyRs displayed punctate forms in both cell types. HL-1 cells significantly varied in their shapes and sizes, such that they were 2- to 3-fold shorter (length:  $36.8 \pm 1.2 \mu\text{m}$ ,  $n = 122$ ) than intact atrial cells, but more or less similar in mean width ( $16.8 \pm 0.72 \mu\text{m}$ ,  $n = 122$ ) (Fig. 3D). These cells showed regular autorhythmic beating at  $> \sim 70\%$  confluence (Fig. 3E;  $97 \pm 12$  beats/min,  $n = 62$ , at 35  $^{\circ}$ C).

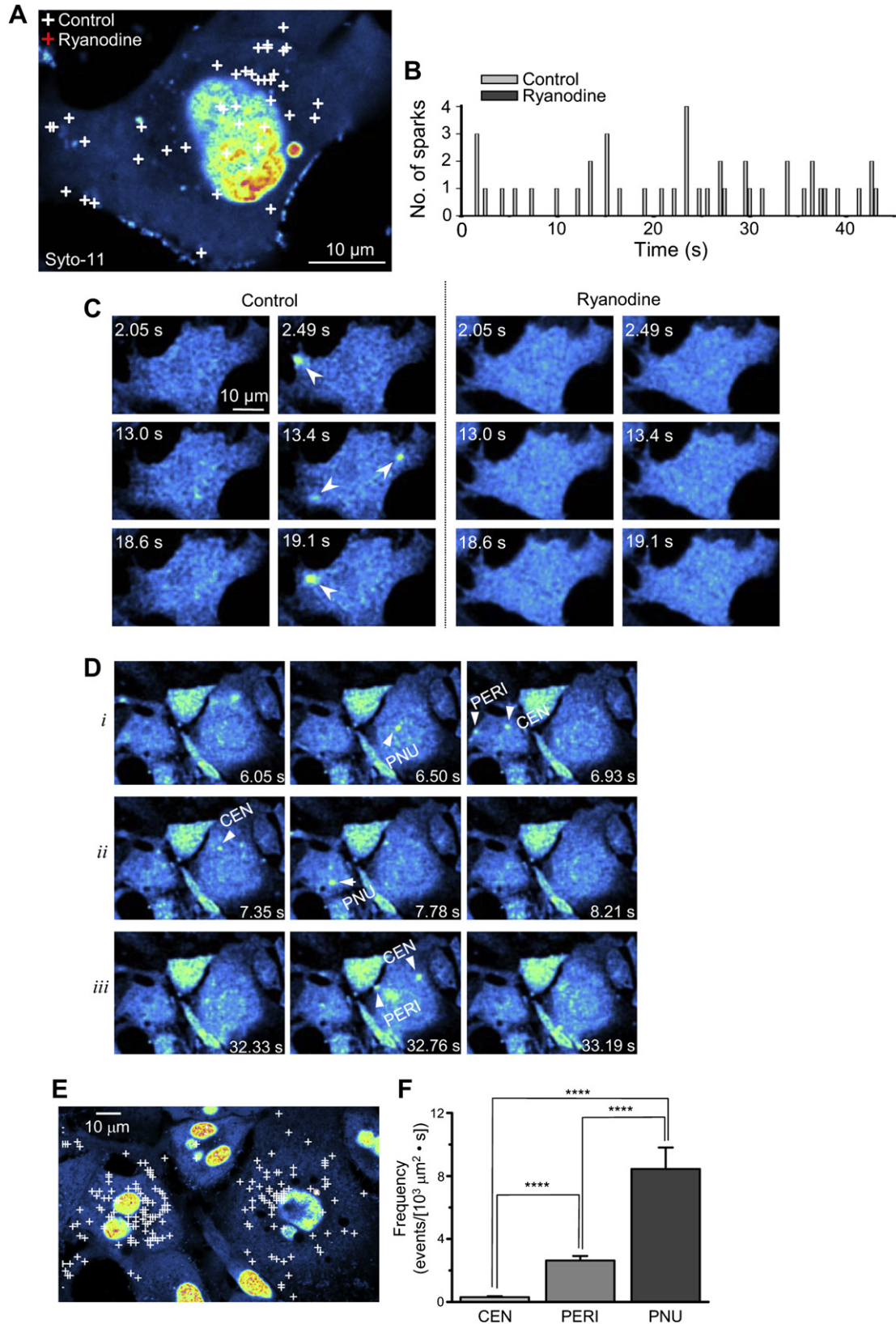
#### 4.2. Characterization of spatio-temporal properties of $\text{Ca}^{2+}$ sparks in HL-1 cells

Consistent with the punctate-form distributions of RyR2 in HL-1 cells (Fig. 3B), we found focal  $\text{Ca}^{2+}$  release events that were completely removed by 20  $\mu\text{M}$  ryanodine (Fig. 4A–C) or by 1 mM tetracaine (data not shown). A low concentration of extracellular  $\text{Ca}^{2+}$  (50  $\mu\text{M}$ ) was used to suppress autorhythmic  $\text{Ca}^{2+}$  transients to record spontaneous  $\text{Ca}^{2+}$  sparks without depleting the SR  $\text{Ca}^{2+}$ . Focal  $\text{Ca}^{2+}$  releases were automatically identified by a computerized algorithm in the *Pic* PC program as described previously. It was found that the  $\text{Ca}^{2+}$  sparks were frequently detected around the nucleus compared with other subcellular area (Fig. 4D and E). The frequency of  $\text{Ca}^{2+}$  sparks was calculated as described earlier for intact atrial cells. The frequency (events/ $[10^3 \mu\text{m}^2 \text{s}]$ ) of the  $\text{Ca}^{2+}$

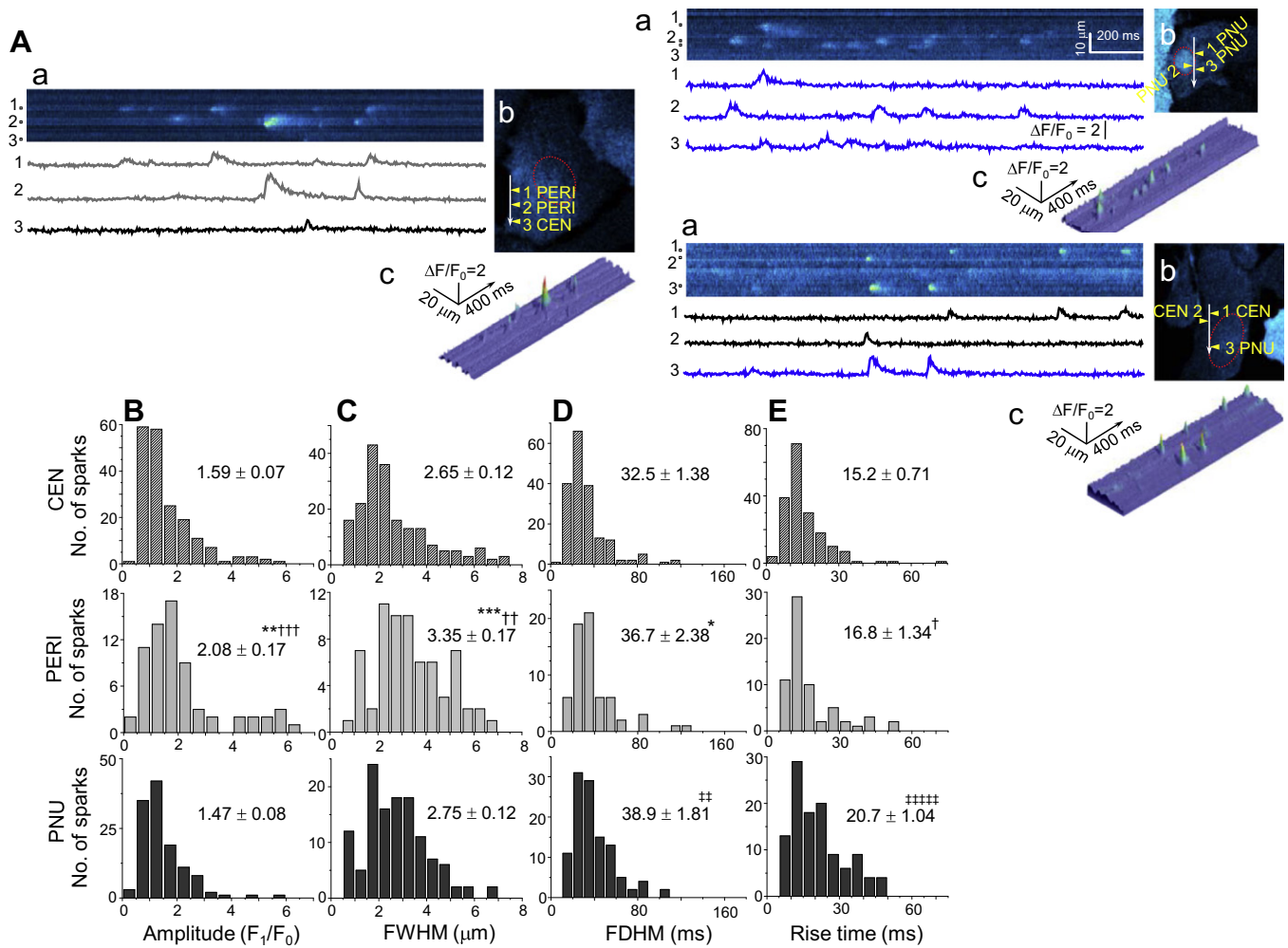
sparks in HL-1 cells was the highest in the peri-nucleus (PNU) ( $\sim 8.5$ ) compared with those measured from other subcellular regions (Fig. 4F), which is different from the largest frequency at the periphery in intact atrial cells (Fig. 2D). The  $\text{Ca}^{2+}$  spark frequency was 8-fold higher in the cell periphery than the center in HL-1 cells (center,  $\sim 0.3$  vs. periphery,  $\sim 2.5$ ; Fig. 4F).

Fig. 5A displays average line-scan images of peripheral, central and peri-nuclear sparks measured at 1.8-ms intervals in HL-1 cells and time courses of single sparks. At the spark center identified by the program, a modified Gaussian fitting (Woo et al., 2003a) was performed along  $y$  (space) axis in a restricted length (7  $\mu\text{m}$ ) of the line-scan image to give the amplitude ( $F_1/F_0$ ) and FWHM. Time course of single spark was measured from the center of the Gaussian curve  $\pm 0.6 \mu\text{m}$  along the  $x$  axis (time), which was used to measure the FDHM and rise time (time-to-90% of peak).

Such detailed analysis on the unitary properties of single sparks showed that peripheral sparks were significantly brighter than the central and peri-nuclear sparks (Fig. 5B and C), which is consistent with the properties of peripheral sparks observed in isolated adult atrial cells (Woo et al., 2003a; Sheehan et al., 2006). The reason for the larger spark amplitude (intensity) in the peripheral region is limited space for  $\text{Ca}^{2+}$  diffusion because of the cell membrane. This limitation results in more rapid expansion in space (larger width) and in larger  $\text{Ca}^{2+}$  concentration (mol/volume) in the junctional



**Fig. 4.** Occurrences of  $\text{Ca}^{2+}$  sparks in HL-1 cells and their frequency in the center, periphery and peri-nucleus. (A) Confocal fluorescence image of HL-1 cell stained with syto-11, the nuclear dye. The cross marks indicate the positions of centers of focal  $\text{Ca}^{2+}$  releases that were automatically detected by computer program (own PC program "Pic 5.14" written in C++) before (white) and after (red) the application of 20  $\mu\text{M}$  ryanodine. (B and C) Time course of spark occurrences (B) and three series of representative spark images (arrowheads) measured in the absence (control) and presence of ryanodine at 2.38 Hz. Fluo-4 AM (3  $\mu\text{M}$ ) was loaded for 30 min and excited at 488 nm Ar laser. Fluorescence was detected at  $>510$  nm using laser scanning confocal microscope (NA 1.4, C1, Eclipse Nikon). (D) Series of confocal  $\text{Ca}^{2+}$  images showing representative  $\text{Ca}^{2+}$  sparks detected at periphery, center, and peri-nucleus in HL-1 cells. (E)  $\text{Ca}^{2+}$  release sites (cross) were marked on the syto-11 image. (F) Mean spark frequency in the CEN, PERI, and PNU.  $n = 23$  cells. \*\*\*\* $P < 0.0001$  between two groups.



**Fig. 5.** Parametric profiles of central, peripheral and peri-nuclear sparks in HL-1 cells. (A-a) Confocal line-scan images measured at 1.8-ms intervals by the repetitive scanning (C1 model, Nikon) of the line shown in A-b (upper), and time courses ( $F/F_0$ ) of numbered sparks (lower). The traces were generated by time-dependent averaging of fluorescence from the local regions marked by the hollow boxes. (A-b) Position of the scanning line in the cell and locations (arrowheads) of sparks (“1–3”) shown below the line-scan image. Red circle indicates the position of nucleus. (A-c) surface plot of the line-scan image. PERI, CEN, and PNU indicate peripheral, central and peri-nuclear sparks, respectively. (B–E) Histograms of  $\text{Ca}^{2+}$  spark peak amplitude ( $\Delta F_1/F_0$ ; B), full width at half maximal amplitude (FWHM, measured at peak area; C), full duration at half maximal amplitude (FDHM; D), and rise time (E). Data were represented as mean  $\pm$  SEM.  $n = 28$  cells. \*CEN ( $n = 190$ ) vs. PERI ( $n = 68$ ). †PERI vs. PNU ( $n = 123$ ). ‡CEN vs. PNU.

space at the same amount of  $\text{Ca}^{2+}$  release. Peri-nuclear sparks lasted longer (Fig. 5D) and developed more slowly than central or peripheral sparks (Fig. 5E). Peripheral and peri-nuclear  $\text{Ca}^{2+}$  sparks were often repetitively activated from the same spots, suggesting distinct regulatory mechanism for the activation of peripheral and peri-nuclear sparks. Long-lasting property and smaller amplitude of peri-nuclear sparks in HL-1 cells are very similar to those in isolated rat atrial myocytes. Overall magnitudes of HL-1 cell sparks were somewhat larger than those observed in intact atrial cells. These results indicate that characteristics of  $\text{Ca}^{2+}$  sparks at junctional, non-junctional, and peri-nuclear regions are maintained in HL-1 cells even with somewhat different sizes.

#### 4.3. Loss of peri-nuclear $\text{Ca}^{2+}$ sparks in $\text{IP}_3\text{R1}$ knock-down HL-1 cells

To understand the reason for the high frequency of peri-nuclear  $\text{Ca}^{2+}$  sparks in HL-1 cells, we measured the SR  $\text{Ca}^{2+}$  loading status in the periphery, center, and peri-nucleus using 10 mM caffeine, because the SR luminal  $\text{Ca}^{2+}$  may increase the sensitivity of RyRs to  $\text{Ca}^{2+}$  (Györke and Györke, 1998). The magnitudes ( $\Delta F/F_0$ ) of caffeine (10 mM)-induced  $\text{Ca}^{2+}$  transients were slightly larger in the peri-nucleus ( $2.94 \pm 0.15$ ) than the periphery ( $2.71 \pm 0.23$ ) or center

( $2.73 \pm 0.22$ ;  $n = 12$ ,  $P < 0.05$ , PNU vs. PERI or CEN). The slight difference in the SR  $\text{Ca}^{2+}$  content, however, may not fully explain  $\sim 9$ -fold higher spark frequency in the peri-nuclear compartment. Because  $\text{IP}_3\text{R1}$  was highly expressed around the nucleus in HL-1 cells (Kim et al., in press) (Fig. 6C, Ad-Con), we tested if  $\text{IP}_3\text{R1}$  is involved in the regulation of peri-nuclear sparks using genetic knock-down (KD) of  $\text{IP}_3\text{R1}$ . After screening several candidate siRNAs (AccuTarget™ Genome-wide pre-designed siRNA, Bioneer, Korea) for  $\text{IP}_3\text{R1}$  KD, we could find the siRNA sequence [sense GGAGGGAUCUACGAAUGGA (dTdT), and antisense UCCAUCUGAUAUCCUCC (dTdT)] that significantly inhibits  $\text{IP}_3\text{R1}$  expression by  $>90\%$  (Fig. 6A). Based on the siRNA sequence, shRNA was constructed to insert into the adenoviral vector system (Adeno-X™ ViraTrak™ DsRed-Express Expression System 2, Clontech). Western blotting and immunostaining in HL-1 cells, infected by control adenovirus only (Ad-con, WT) and by the shRNA-containing adenovirus (Ad- $\text{IP}_3\text{R1}$ ), showed  $\geq 90\%$  KD of  $\text{IP}_3\text{R1}$  after 2 days of incubation (Fig. 6B and C). There was no significant change in the frequency and unitary properties of  $\text{Ca}^{2+}$  sparks by the infection of adenovirus only (data not shown).

Interestingly, we found that the frequency of spontaneous peri-nuclear  $\text{Ca}^{2+}$  sparks was reduced to  $\approx 10\%$  in  $\text{IP}_3\text{R1}$  KD cells (Fig. 7A–C). The occurrence of central sparks was also decreased

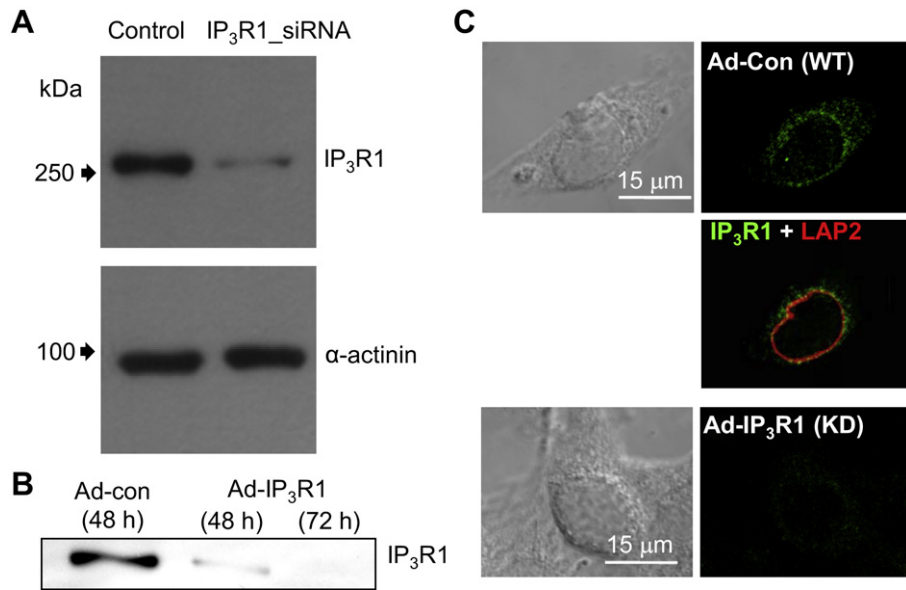


**Fig. 6.** siRNA and adenovirus mediated IP<sub>3</sub>R1 knock-down (KD) in HL-1 cells. Representative immunoblots showing IP<sub>3</sub>R1 KD in HL-1 cells after transfection with siRNA (A) and after infection with adenovirus targeting IP<sub>3</sub>R1 mRNA (B). (A) Cells were either transfected with control siRNA (*control*) or with siRNA directed against IP<sub>3</sub>R1 (*IP<sub>3</sub>R1\_siRNA*).  $\alpha$ -actinin was used as a loading control. (B) Cells were either infected with control adenovirus (*Ad-con*), or with adenovirus targeting IP<sub>3</sub>R1 (*Ad-IP<sub>3</sub>R1*). Total protein was prepared from the cells 48 h post transfection for siRNA experiments, and 48 and 72 h post infection for adenoviral experiments. 50  $\mu$ g of total protein was run on a 5% SDS-polyacrylamide gel and the blots were sequentially probed with isoform specific IP<sub>3</sub>R antibodies and  $\alpha$ -actinin antibody. (C) Comparison of IP<sub>3</sub>R1 immunoreactivity between WT (*green*) and IP<sub>3</sub>R1 KD cells. Superimposition of IP<sub>3</sub>R1 (*green*) and inner nuclear membrane protein LAP2 (*red*) showed that IP<sub>3</sub>R1 was co-localized with LAP2 (*IP<sub>3</sub>R1 + LAP2*, middle panel, *yellow*).

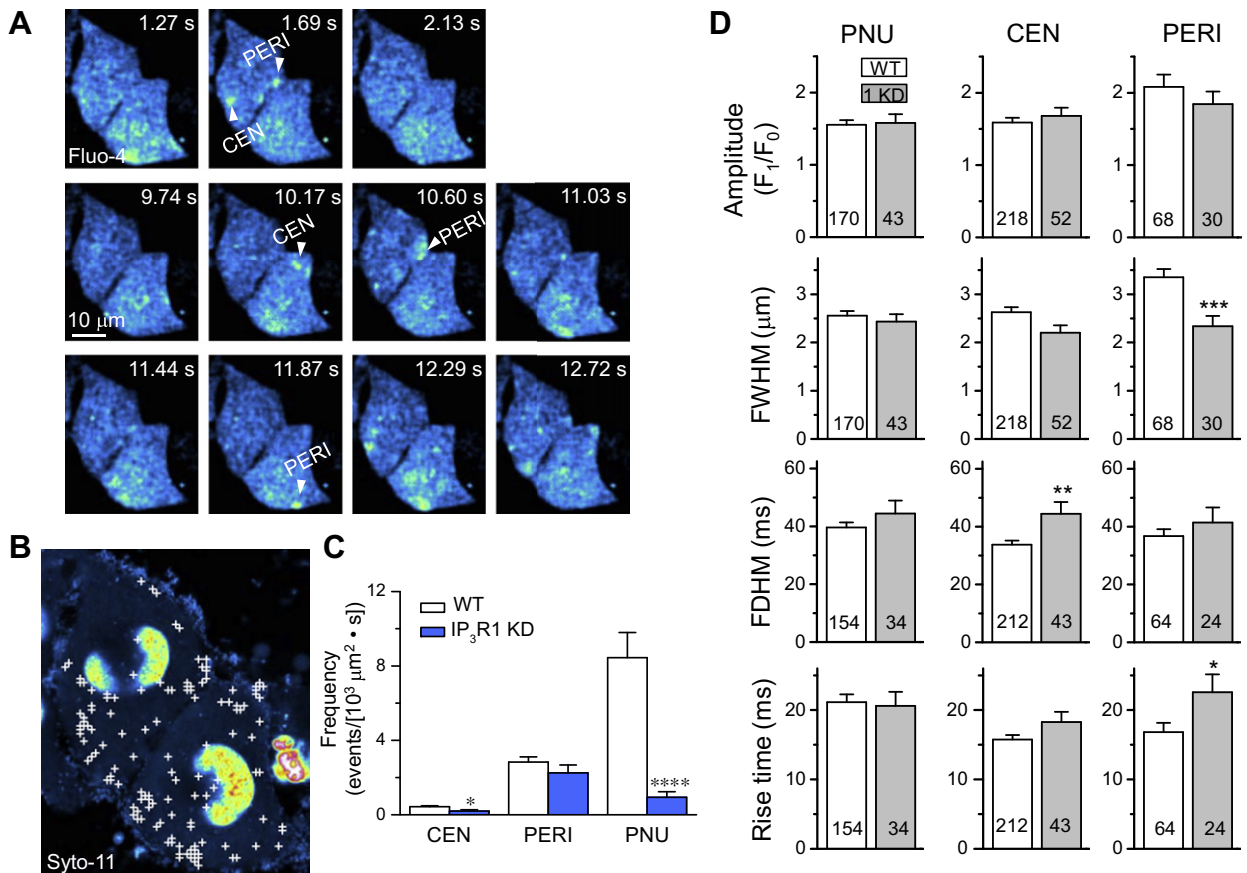


**Fig. 7.** Suppression of peri-nuclear Ca<sup>2+</sup> sparks by IP<sub>3</sub>R1 KD in HL-1 cells. (A) Series of confocal Ca<sup>2+</sup> images (2.38 Hz) showing Ca<sup>2+</sup> sparks in the center (CEN), periphery (PERI), and peri-nucleus (PNU) in IP<sub>3</sub>R1 KD HL-1 cells. (B) Map of spark sites superimposed on the syto-11 fluorescence image. (C) Comparison of mean spark frequency between WT and IP<sub>3</sub>R1 KD. \**P* < 0.05, \*\*\*\**P* < 0.0001, WT (*n* = 12) vs. IP<sub>3</sub>R1 KD (*n* = 14). (D) Comparisons of mean amplitude, FWHM, FDHM, and rise time between WT and IP<sub>3</sub>R1 KD ("1 KD") cells. Numbers in each column indicate the number of sparks analyzed. \**P* < 0.05, \*\**P* < 0.01, \*\*\**P* < 0.001, WT vs. KD.

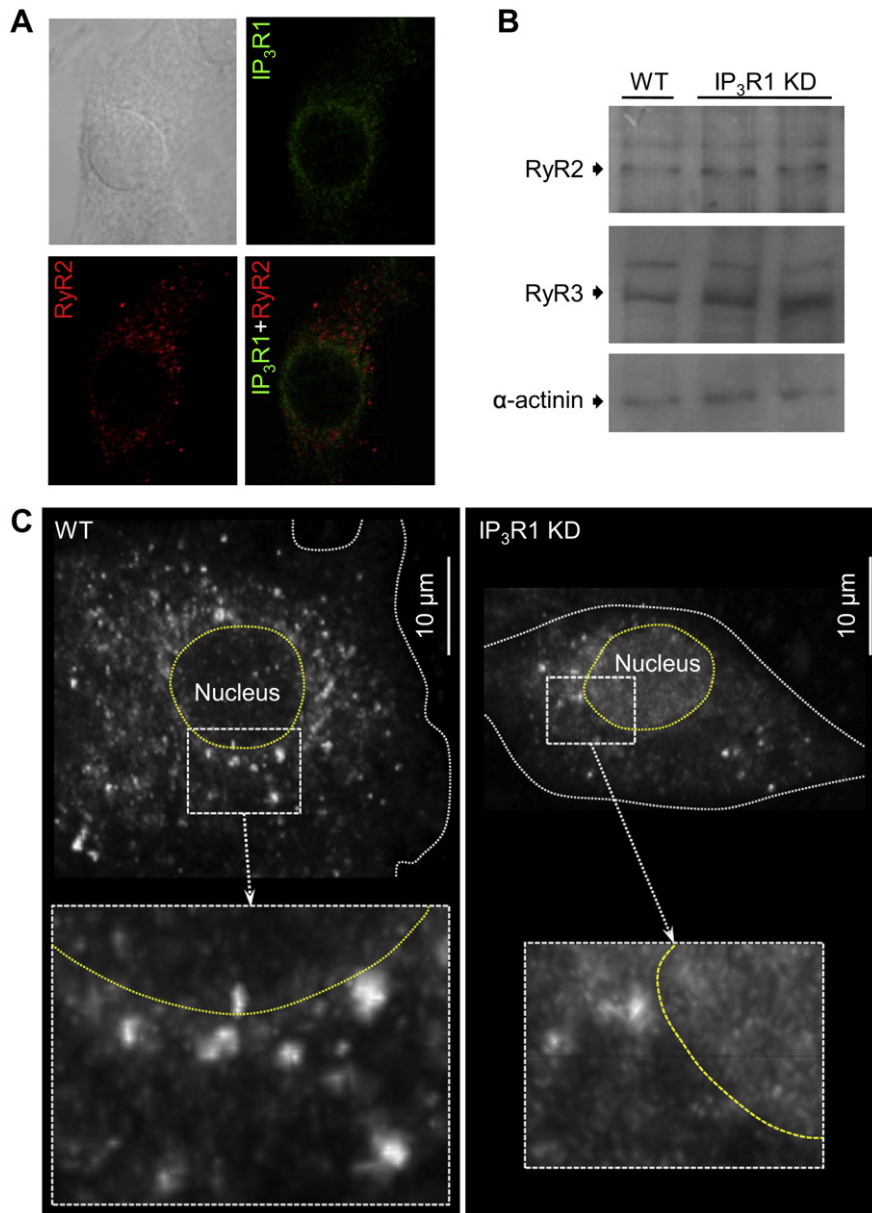


**Fig. 8.** Reduction of peri-nuclear RyR2 clusters by IP<sub>3</sub>R1 KD in HL-1 cells. (A) Confocal immunofluorescence images for IP<sub>3</sub>R1 (green) and RyR2 (red), and superimposition of the two immunofluorescence images (IP<sub>3</sub>R1 + RyR2). Antibodies for RyR2, RyR3, and IP<sub>3</sub>R1 were purchased from Chemicon (USA). (B) Comparison of protein expressions of RyR2 (~550 kD) and RyR3 (~550 kD) between WT and IP<sub>3</sub>R1 KD HL-1 cells. (C) Three-dimensional images of RyR2 immunofluorescence, reconstructed from z-directional confocal sectioning, in WT and IP<sub>3</sub>R1 KD HL-1 cells. Position of the nucleus was marked by yellow dots. Lower panel shows magnified images from the boxed regions in the upper panel.

by 2-fold in IP<sub>3</sub>R1 KD cells, while that of peripheral sparks was not significantly changed by IP<sub>3</sub>R1 KD (Fig. 7C). Analysis on the unitary properties of single sparks and time course showed that the amplitude, width, duration and rise time of residual Ca<sup>2+</sup> sparks in the peri-nucleus of IP<sub>3</sub>R1-KD cells were similar to those in WT cells (Fig. 7D). Duration of central Ca<sup>2+</sup> sparks was prolonged by IP<sub>3</sub>R1 KD (Fig. 7D, FDHM). Peripheral sparks in IP<sub>3</sub>R1 KD cells were narrower and more slowly grew than those in WT cells (Fig. 7D).

#### 4.4. Possible role of IP<sub>3</sub>R1 in RyR clustering in atrial cells

In the next series of experiments, we investigated the mechanisms for the suppression of peri-nuclear Ca<sup>2+</sup> sparks by IP<sub>3</sub>R1 KD. Caffeine (10 mM)-induced Ca<sup>2+</sup> transients ( $\Delta F/F_0$ ) in the peri-

nucleus were slightly decreased by IP<sub>3</sub>R1 KD (WT,  $2.5 \pm 0.4$ ,  $n = 22$ ; KD,  $1.8 \pm 0.1$ ,  $n = 14$ ,  $P < 0.05$ ,  $n = 11$ ), whereas they were not changed by IP<sub>3</sub>R1 KD in the periphery (WT,  $2.3 \pm 0.3$ ; KD,  $2.2 \pm 0.2$ ,  $P > 0.05$ ). Although a decrease in the peri-nuclear SR Ca<sup>2+</sup> loading by IP<sub>3</sub>R1 KD is consistent with lower frequency of peri-nuclear sparks observed in IP<sub>3</sub>R1 KD cells, it may not fully explain the effect of IP<sub>3</sub>R1 KD on the frequency of peri-nuclear sparks.

It has been recently suggested that wide long-lasting Ca<sup>2+</sup> release events in specific peri-nuclear regions in canine Purkinje cells are evoked by co-localized RyRs and IP<sub>3</sub>Rs (Hirose et al., 2008). Such possibility was also tested by co-immunolocalization using the antibodies specific to the RyR2 and IP<sub>3</sub>R1 in the same HL-1 cells. We were unable to find any co-localizations of RyR2 and IP<sub>3</sub>R1 (see no yellow fluorescence; Fig. 8A). These results suggest that a direct interaction between IP<sub>3</sub>R1 and RyR2 is not likely to occur in the

peri-nucleus of HL-1 cells and that such mechanism cannot explain the significantly high occurrence of peri-nuclear  $\text{Ca}^{2+}$  sparks in control HL-1 cells.

We tested the hypothesis that nuclear  $\text{IP}_3\text{R1}$  regulates the level of RyR protein by controlling gene expression using Western blotting experiment. The level of RyR2 was similar between WT and  $\text{IP}_3\text{R1}$  KD HL-1 cells (Fig. 8B). However, the level of RyR3 was slightly enhanced by  $\text{IP}_3\text{R1}$  KD (Fig. 8B). RyR1 was not detected in both WT and KD cells. Interestingly, immunostaining of RyR2 with specific antibodies revealed a significant loss of punctate-form RyR2 immunofluorescence around the nucleus in  $\text{IP}_3\text{R1}$  KD cells compared with WT cells (Fig. 8C). There was some level of decrease in the RyR2 punctate fluorescence in the central zone of  $\text{IP}_3\text{R1}$  KD HL-1 cells. These results indicate that  $\text{IP}_3\text{R1}$  KD may inhibit the formation of RyRs-clusters in the peri-nucleus and center of HL-1 cells. The loss of RyR2 clusters may prevent the development of  $\text{Ca}^{2+}$  sparks. In addition, the slight changes in the unitary properties of central and peripheral sparks by  $\text{IP}_3\text{R1}$  KD may be related to the alterations in the extent of RyR clustering. These evidences provide a novel insight into a possible role of peri-nuclear  $\text{IP}_3\text{R1}$  in the posttranslational clustering of RyR2 in atrial myocytes.

## 5. Conclusions and future perspectives

High-speed and 2D confocal  $\text{Ca}^{2+}$  imaging has advanced our knowledge on the local aspects of atrial  $\text{Ca}^{2+}$  signaling in atrial myocytes over the last decade. The unique ultrastructure of atrial myocytes and their distinct context of  $\text{Ca}^{2+}$  regulatory proteins may explain spatio-temporal characteristics of  $\text{Ca}^{2+}$  sparks and  $\text{Ca}^{2+}$  waves under physiological and pathological conditions. Although central  $\text{Ca}^{2+}$  release in atrial myocytes plays a critical role in activating the myofilaments, the mechanisms by which these sites are triggered and regulated remain largely unknown. It remains a possibility that other regulatory mechanisms in the SR or mitochondria can control the speed or magnitude of  $\text{I}_{\text{Ca}}$ -triggered  $\text{Ca}^{2+}$  propagation wave. It may be instructive to further examine the possibility of peri-nuclear  $\text{Ca}^{2+}$  sparks responsible for controlling gene transcription in atrial myocytes.

Advances in our understanding of  $\text{IP}_3\text{R}$  signaling demonstrate that  $\text{IP}_3\text{Rs}$  are important regulator of atrial  $\text{Ca}^{2+}$  signaling. The physiological roles of  $\text{IP}_3\text{Rs}$ , however, are not fully understood and need to be determined in more detail. Specific KD of different  $\text{IP}_3\text{R}$  subtypes using intact atrial myocytes combined with detailed subcellular-level physiological studies will provide essential information on the role of each subtype in atrial cell functions. Our experimental results in adult atrial cell line may provide theoretical and methodological bases for further determination of the role of  $\text{IP}_3\text{R}$  subtypes in the regulation of physiological local  $\text{Ca}^{2+}$  signaling in intact cardiac cells. The mechanisms by which atrial  $\text{IP}_3\text{R1}$  regulate posttranslational clustering of RyR2 in the peri-nuclear and central SR remain to be answered.

## Acknowledgements

This work was supported by Korea Science and Engineering Foundation grant funded by the Korea Government (MOST) (No. 2009-0053266) and in part by grant from Korea Ministry of Science and Technology (M10503010001-08N030100113). We thank W. Claycomb for HL-1 cells.

## References

Ayettey, A.S., Navaratnam, V., 1978. The T-tubule system in the specialized and general myocardium of the rat. *J. Anat.* 127, 125–140.

- Bare, D.J., Kettlun, C.S., Liang, M., Bers, D.M., Mignery, G.A., 2005. Cardiac type 2 inositol 1,4,5-trisphosphate receptor: interaction and modulation by calcium/calmodulin-dependent protein kinase II. *J. Biol. Chem.* 280, 15912–15920.
- Berlin, J.R., 1995. Spatiotemporal changes of  $\text{Ca}^{2+}$  during electrically evoked contractions in atrial and ventricular cells. *Am. J. Physiol.* 269, H1165–H1170.
- Berridge, M.J., 2006. Remodelling  $\text{Ca}^{2+}$  signalling systems and cardiac hypertrophy. *Biochem. Soc. Trans.* 34, 228–231.
- Berridge, M.J., 2009. Inositol trisphosphate and calcium signalling mechanisms. *Biochim. Biophys. Acta* 1793, 933–940.
- Beuckelmann, D.J., Wier, W.G., 1988. Mechanism of release of calcium from sarcoplasmic reticulum of guinea-pig cardiac cells. *J. Physiol.* 405, 233–255.
- Bezprozvanny, I., Watras, J., Ehrlich, B.E., 1991. Bell-shaped calcium-response curves of  $\text{Ins}(1,4,5)\text{P}_3$ - and calcium-gated channels from endoplasmic reticulum of cerebellum. *Nature* 351, 751–754.
- Cannell, M.B., Cheng, H., Lederer, W.J., 1994. Spatial non-uniformities in  $[\text{Ca}^{2+}]_i$  during excitation-contraction coupling in cardiac myocytes. *Biophys. J.* 67, 1942–1956.
- Carl, S.L., Felix, K., Caswell, A.H., Brandt, N.R., Ball Jr., W.J., Vaghy, P.L., Meissner, G., Ferguson, D.G., 1995. Immunolocalization of sarcolemmal dihydropyridine receptor and sarcoplasmic reticular triadin and ryanodine receptor in rabbit ventricle and atrium. *J. Cell Biol.* 129, 673–682.
- Cheng, H., Lederer, W.J., Cannell, M.B., 1993. Calcium sparks: elementary events underlying excitation-contraction coupling in heart muscle. *Science* 262 (5134), 740–744.
- Claycomb, W.C., Lanson Jr., N.A., Stallworth, B.S., Egeland, D.B., Delcarpio, J.B., Bahinski, A., Izzo Jr., N.J., 1998. HL-1 cells: a cardiac muscle cell line that contracts and retains phenotypic characteristics of the adult cardiomyocyte. *Proc. Natl. Acad. Sci. U. S. A.* 95, 2979–2984.
- Cleemann, L., Morad, M., 1991. Role of  $\text{Ca}^{2+}$  channel in cardiac excitation-contraction coupling in the rat: evidence from  $\text{Ca}^{2+}$  transients and contraction. *J. Physiol.* 432, 283–312.
- Cleemann, L., Wang, W., Morad, M., 1998. Two-dimensional confocal images of organization, density, and gating of focal  $\text{Ca}^{2+}$  release sites in rat cardiac myocytes. *Proc. Natl. Acad. Sci. U. S. A.* 95, 10984–10989.
- Finch, E.A., Turner, T.J., Goldin, S.M., 1991. Calcium as a coagonist of inositol 1,4,5-trisphosphate-induced calcium release. *Science* 252, 443–446.
- Forssmann, W.G., Girardier, L., 1970. A study of the T system in rat heart. *J. Cell Biol.* 44, 1–19.
- Go, L.O., Moschella, M.C., Watras, J., Handa, K.K., Fyfe, B.S., Marks, A.R., 1995. Differential regulation of two types of intracellular calcium release channels during end-stage heart failure. *J. Clin. Invest.* 95, 888–894.
- Gorza, L., Schiaffino, S., Volpe, P., 1993. Inositol 1,4,5-trisphosphate receptor in heart: evidence for its concentration in Purkinje myocytes of the conduction system. *J. Cell Biol.* 121, 345–353.
- Goutsouliak, V., Rabkin, S.W., 1997. Angiotensin II-induced inositol phosphate generation is mediated through tyrosine kinase pathways in cardiomyocytes. *Cell. Signal.* 9, 505–512.
- Györke, I., Györke, S., 1998. Regulation of the cardiac ryanodine receptor channel by luminal  $\text{Ca}^{2+}$  involves luminal  $\text{Ca}^{2+}$  sensing sites. *Biophys. J.* 75, 2801–2810.
- Hatem, S.N., Bénardeau, A., Rucker-Martin, C., Marty, I., de Chamisso, P., Villaz, M., Mercadier, J.J., 1997. Different compartments of sarcoplasmic reticulum participate in the excitation-contraction coupling process in human atrial myocytes. *Circ. Res.* 80, 345–353.
- Hilal-Dandan, R., Urasawa, K., Brunton, L.L., 1992. Endothelin inhibits adenylate cyclase and stimulates phosphoinositide hydrolysis in adult cardiac myocytes. *J. Biol. Chem.* 267, 10620–10624.
- Hirose, M., Stuyvers, B., Dun, W., Ter Keurs, H., Boyden, P.A., 2008. Wide long lasting perinuclear  $\text{Ca}^{2+}$  release events generated by an interaction between ryanodine and  $\text{IP}_3$  receptors in canine Purkinje cells. *J. Mol. Cell. Cardiol.* 45, 176–184.
- Hove-Madsen, L., Llach, A., Bayes-Genis, A., Roura, S., Rodríguez Font, E., Aris, A., Cinca, J., 2004. Atrial fibrillation is associated with increased spontaneous calcium release from the sarcoplasmic reticulum in human atrial myocytes. *Circulation* 110, 1358–1363.
- Hüser, J., Lipsius, S.L., Blatter, L.A., 1996. Calcium gradients during excitation-contraction coupling in cat atrial myocytes. *J. Physiol.* 494 (Pt 3), 641–651.
- Iino, M., 1990. Biphasic  $\text{Ca}^{2+}$  dependence of inositol 1,4,5-trisphosphate-induced  $\text{Ca}^{2+}$  release in smooth muscle cells of the guinea pig taenia caeci. *J. Gen. Physiol.* 95, 1103–1122.
- Kim, J.C., Son, M.J., Subedi, K.P., Kim, D.H., Woo, S.H.  $\text{IP}_3$ -induced cytosolic and nuclear  $\text{Ca}^{2+}$  signals in HL-1 atrial myocytes: possible role of  $\text{IP}_3$  receptor subtypes. *Mol. Cells*, in press.
- Kirk, M.M., Izu, L.T., Chen-Izu, Y., McCulle, S.L., Wier, W.G., Balke, C.W., Shorofsky, S.R., 2003. Role of the transverse-axial tubule system in generating calcium sparks and calcium transients in rat atrial myocytes. *J. Physiol.* 547, 441–451.
- Kockskämper, J., Sheehan, K.A., Bare, D.J., Lipsius, S.L., Mignery, G.A., Blatter, L.A., 2001. Activation and propagation of  $\text{Ca}^{2+}$  release during excitation-contraction coupling in atrial myocytes. *Biophys. J.* 81, 2590–2605.
- Kockskämper, J., Seidlmayer, L., Walther, S., Hellenkamp, K., Maier, L.S., Pieske, B., 2008. Endothelin-1 enhances nuclear  $\text{Ca}^{2+}$  transients in atrial myocytes through  $\text{Ins}(1,4,5)\text{P}_3$ -dependent  $\text{Ca}^{2+}$  release from perinuclear  $\text{Ca}^{2+}$  stores. *J. Cell Sci.* 121, 186–195.
- Lederer, W.J., Tsien, R.W., 1976. Transient inward current underlying arrhythmogenic effects of cardiotonic steroids in Purkinje fibres. *J. Physiol.* 263, 73–100.

- Li, X., Zima, A.V., Sheikh, F., Blatter, L.A., Chen, J., 2005. Endothelin-1-induced arrhythmogenic  $Ca^{2+}$  signaling is abolished in atrial myocytes of inositol-1,4,5-trisphosphate ( $IP_3$ )-receptor type 2-deficient mice. *Circ. Res.* 96, 1274–1281.
- Lipp, P., Laine, M., Tovey, S.C., Burrell, K.M., Berridge, M.J., Li, W., Bootman, M.D., 2000. Functional  $InsP_3$  receptors that may modulate excitation–contraction coupling in the heart. *Curr. Biol.* 10, 939–942.
- Lipp, P., Pott, L., 1988a. Transient inward current in guinea-pig atrial myocytes reflects a change of sodium–calcium exchange current. *J. Physiol.* 397, 601–630.
- Lipp, P., Pott, L., 1988b. Voltage dependence of sodium–calcium exchange current in guinea-pig atrial myocytes determined by means of an inhibitor. *J. Physiol.* 403, 355–366.
- Lipsius, S.L., Hüser, J., Blatter, L.A., 2001. Intracellular  $Ca^{2+}$  release sparks atrial pacemaker activity. *News Physiol. Sci.* 16, 101–106.
- Luo, D., Yang, D., Lan, X., Li, K., Li, X., Chen, J., Zhang, Y., Xiao, R.P., Han, Q., Cheng, H., 2008. Nuclear  $Ca^{2+}$  sparks and waves mediated by inositol 1,4,5-trisphosphate receptors in neonatal rat cardiomyocytes. *Cell Calcium* 43, 165–174.
- Mackenzie, L., Bootman, M.D., Berridge, M.J., Lipp, P., 2001. Predetermined recruitment of calcium release sites underlies excitation–contraction coupling in rat atrial myocytes. *J. Physiol.* 530, 417–429.
- Mackenzie, L., Bootman, M.D., Laine, M., Berridge, M.J., Thuring, J., Holmes, A., Li, W.H., Lipp, P., 2002. The role of inositol 1,4,5-trisphosphate receptors in  $Ca^{2+}$  signalling and the generation of arrhythmias in rat atrial myocytes. *J. Physiol.* 541, 395–409.
- Mohler, P.J., Davis, J.Q., Bennett, V., 2005. Ankyrin-B coordinates the Na/K ATPase, Na/Ca exchanger, and  $InsP_3$  receptor in a cardiac T-tubule/SR microdomain. *PLoS Biol.* 3, 2158–2167.
- Näbauer, M., Ellis-Davies, G.C., Kaplan, J.H., Morad, M., 1989. Modulation of  $Ca^{2+}$  channel selectivity and cardiac contraction by photorelease of  $Ca^{2+}$ . *Am. J. Physiol.* 256, H916–H920.
- Niggli, E., Lederer, W.J., 1990. Voltage-independent calcium release in heart muscle. *Science* 250, 565–568.
- Parker, A.K., Gergely, F.V., Taylor, C.W., 2004. Targeting of inositol 1,4,5-trisphosphate receptors to the endoplasmic reticulum by multiple signals within their transmembrane domains. *J. Biol. Chem.* 279, 23797–23805.
- Pucéat, M., Vassort, G., 1996. Purinergic stimulation of rat cardiomyocytes induces tyrosine phosphorylation and membrane association of phospholipase C  $\gamma$ : a major mechanism for  $InsP_3$  generation. *Biochem. J.* 318, 723–728.
- Sartiani, L., Bochet, P., Cerbai, E., Mugelli, A., Fischmeister, R., 2002. Functional expression of the hyperpolarization-activated, non-selective cation current  $I_f$  in immortalized HL-1 cardiomyocytes. *J. Physiol.* 545, 81–92.
- Sheehan, K.A., Blatter, L.A., 2003. Regulation of junctional and non-junctional sarcoplasmic reticulum calcium release in excitation–contraction coupling in cat atrial myocytes. *J. Physiol.* 546, 119–135.
- Sheehan, K.A., Zima, A.V., Blatter, L.A., 2006. Regional differences in spontaneous  $Ca^{2+}$  spark activity and regulation in cat atrial myocytes. *J. Physiol.* 572, 799–809.
- Soldatov, N.M., 2003.  $Ca^{2+}$  channel moving tail: link between  $Ca^{2+}$ -induced inactivation and  $Ca^{2+}$  signal transduction. *Trends Pharmacol. Sci.* 24, 167–171.
- Sommer, J.R., Waugh, R.A., 1976. The ultrastructure of the mammalian cardiac muscle cell—with special emphasis on the tubular membrane systems. A review. *Am. J. Pathol.* 82, 192–232.
- Streb, H., Irvine, R.F., Berridge, M.J., Schulz, I., 1983. Release of  $Ca^{2+}$  from a non-mitochondrial intracellular store in pancreatic acinar cells by inositol-1,4,5-trisphosphate. *Nature* 306, 67–69.
- Thu, L.T., Ahn, J.R., Woo, S.H., 2006. Inhibition of L-type  $Ca^{2+}$  channel by mitochondrial  $Na^+$ – $Ca^{2+}$  exchange inhibitor CGP-37157 in rat atrial myocytes. *Eur. J. Pharmacol.* 552, 15–19.
- Wier, W.G., Egan, T.M., López-López, J.R., Balke, C.W., 1994. Local control of excitation–contraction coupling in rat heart cells. *J. Physiol.* 474, 463–471.
- Woo, S.H., Cleemann, L., Morad, M., 2002.  $Ca^{2+}$  current-gated focal and local  $Ca^{2+}$  release in rat atrial myocytes: evidence from rapid 2-D confocal imaging. *J. Physiol.* 543, 439–453.
- Woo, S.H., Cleemann, L., Morad, M., 2003a. Spatiotemporal characteristics of junctional and nonjunctional focal  $Ca^{2+}$  release in rat atrial myocytes. *Circ. Res.* 92, e1–e11.
- Woo, S.H., Soldatov, N.M., Morad, M., 2003b. Modulation of  $Ca^{2+}$  signalling in rat atrial myocytes: possible role of the alpha1C carboxyl terminal. *J. Physiol.* 552, 437–447.
- Woo, S.H., Cleemann, L., Morad, M., 2005. Diversity of atrial local  $Ca^{2+}$  signalling: evidence from 2-D confocal imaging in  $Ca^{2+}$ -buffered rat atrial myocytes. *J. Physiol.* 567, 905–921.
- Woodcock, E.A., Matkovich, S.J., 2005.  $Ins(1,4,5)P_3$  receptors and inositol phosphates in the heart—evolutionary artifacts or active signal transducers? *Pharmacol. Ther.* 107, 240–251.
- Yamada, J., Fujimori, K., Ishida, T., Sanpei, M., Honda, S., Sato, A., 2001. Up-regulation of inositol 1,4,5 trisphosphate receptor expression in atrial tissue in patients with chronic atrial fibrillation. *J. Am. Coll. Cardiol.* 37, 1111–1119.
- Zima, A.V., Bare, D.J., Mignery, G.A., Blatter, L.A., 2007.  $IP_3$ -dependent nuclear  $Ca^{2+}$  signalling in the mammalian heart. *J. Physiol.* 584, 601–611.
- Zima, A.V., Blatter, L.A., 2004. Inositol-1,4,5-trisphosphate-dependent  $Ca^{2+}$  signalling in cat atrial excitation–contraction coupling and arrhythmias. *J. Physiol.* 555, 607–615.